The 6th Saudi Engineering Conference, KFUPM, Dhahran, December 2002 Vol. 5. 423

COMBINED CYCLE DYNAMICS

F. M. Mansour[1], A. M. Abdul Aziz[2], S. M. Abdel-Ghany[3], H. M. El-shaer[4]

1: Assistant professor, Power plants Projects Manager, Egyptian Electricity Holding Co.
2: Associate professor, Ain Shams University, Cairo
3: Professor, Ain Shams University, Cairo
4: Chairman of Electric Power Systems Engineering Co. (EPS)

ABSTRACT

A mathematical model describing the dynamic behaviour of each major component of the combined cycle is presented. The formulae were deduced from continuity, momentum, energy, and state equations. P.D.Es were discretized to algebraic equations by using the implicit backward-central finite difference scheme and then solved by iteration. Explicit-Euler's integration method was applied to other D.Es. A multi-element control system was implemented to investigate its effect on the combined cycle's dynamic response. The results obtained were compared with the design and steady state operational data of the unit number 4 in Cairo South Combined Cycle Power Plant showing good agreement. The dynamic results proved the effectiveness of the multi-element control strategy to control the combined cycle plant with fast settling time, neglected steady state error and moderate overshoot or undershoot while assuring a stable operation under sudden changes of load.

Keywords: *Combined cycle, steam power plant, mathematical modeling, dynamic response, heat recovery steam generator, control.*

الملخص

يقدم البحث نموذجاً رياضياً للأداء الديناميكي للأجزاء الرئيسية في الدورة المركبة. وقد استنتجت المعادلات الحاكمة من معادلات الانسيابية وكمية الحركة والطاقة والحالة. ولقد استخدمت طريقة الفوارق المحددة لتحويل المعادلات التفاضلية الجزئية إلى معادلات جبرية بينما استخدمت طريقة أويلر في حالة المعادلات التفاضلية الكلية. ولقد درس تأثير استخدام نظام التحكم ذي العناصر المتعددة على الأداء الزمني للدورة المركبة. ومن مقارنة النتائج العملية المسجلة من الوحدة المركبة الرابعة بمحطة جنوب القاهرة بنتائج النموذج قيد البحث وذلك في حالة الاستقرار ثبت التوافق الجيد بينهما. ولقد أثبت تحليل نتائج الأداء الزمني من خلال النموذج قيد البحث على فاعلية نظام التحكم المقترح ذي العناصر المتعددة في التحكم الجيد في أداء الدورة المركبة وذلك بالإسراع في زمن الاستقرار وتقليل خطأ استقرار الحالة وتقليل الارتفاع والانخفاض المفاجئ للحالة بينما يضمن الوصول إلى تشغيل مستقر في كافة حالات التحميل المفاجئ.

NOMENCLATURE:

A	Area, m^2	$\dot{Q}$	Rate of heat transfer, W
C_p, C_v	Specific heats at constant pressure and volume, J/kg K	r	Radius, m
C_m	Specific heat for metals, J/kg K	R	Radius of gyration, m
d, D	Diameter, m	Re	Reynolds number
E_t	Error as a function of time	s	Specific entropy, J/kg K
f	Friction factor, any function	t	Time, s, thickness, m
g	Gravitational acceleration, m^2/s	T	Temperature, K
h	Heat transfer coefficient, W/m^2K, Enthalpy, J/kg	T_d	Derivative time constant, s
J	Moment of inertia, kg/m^2	T_i	Integral time constant, s
k_p	Proportional gain factor	T_s	Settling time, s
L	Tube length, m, Length, m	u	Specific internal energy, J/kg,
M	Mass, kg		Velocity, m/s
$\dot{m}$	Mass flow rate, kg/s	v	Specific volume, m^3/kg
p	Pressure, bar	V	Volume, m^3
P	Power, W	x	Dryness fraction, x-coordinate
Pr	Prandtle number	y	Level, m, y-coordinate

Greek Symbols

γ	Specific heat ratio C_p/C_v	*fm*	From fluid to metal side
η	Efficiency	*fn*	Fin
λ	Thermal conductivity, W/m K	*fp*	Feed pump
μ	Viscosity, kg/m/s	*g*	Gas, saturated vapour
ρ	Density, kg/m^3	*gd*	Gas damper
ω	Angular velocity, rad/s	*gm*	From gas to metal side
ξ	Entrance loss	*gt*	Gas turbine
		i	Inner

Subscripts

c	Controller	*l*	Load; power demand
comp	Compressor	*m*	Metal
cond	Condenser, conduction	*o*	Outer
dc	Downcomer	*r*	Riser, reference, row
dr	Steam-water drum	*s*	Steam, Superheated steam
ec	Economizer	*st*	Steam turbine
f	Fluid, saturated liquid	*sv*	Steam valve
fg	A change of phase at constant pressure, from fluid to gas side	*w*	Water
		wh	Water header
		wv	Water valve

1. INTRODUCTION

The investigation of the combined cycle dynamics goes in parallel with the investigation of the steam cycle dynamics due to the common components between the two cycles. These investigations were dedicated for developing the cycle design, the control problem, both from operational and economical points of view, and consequently the cycle performance. A summary is given below.

Steam separation in boiler drum was experimentally studied by [Faber, 1951]. The carry over and entrainment were found to increase with increase in load and pressure. Mathematical models of boilers [Chien et al, 1958] and steam generators [Debella et al 1966, Estrada et al, 1964 and Nahavandi et al, 1966] were also developed. Prediction of drum pressure and level as well as their control, was also presented by [Eklund et al, 1973] using perturbation models. In their work, identification of boiler drum dynamics, based on experimental data, was handled through linear and nonlinear models.

Dynamic analysis of heat exchangers was either investigated theoretically [Eigner, 1966], or using the transfer function approach [Schöne, 1966], or using set of governing differential equations [Wang et al, 1991].

Mathematical model of steam power plant under normal and emergency operating conditions was presented by [Usoro et al, 1983]. The methodology was based on lumped parameter approach and the equations were arranged in the state space form to be solved by integration methods like Runge Kutta method. Another approach based on the basic equations of mass, momentum and energy was directed towards the evaluation of the accidental transients in thermal power systems [Mesarovic, 1990]. Advances and drawbacks of the well-known space-time discretization and numerical methods applied to solve the nonlinear equations of heat exchangers in combined cycles were discussed by [Dechamps, 1994]. Software package for steady state behaviour of different elements of power plants was also developed by [Divakaruni et al, 1990]. Dynamic benchmark tests on a number of thermal power plants were also carried out by [Carvalho et al, 1991] to investigate the response time of different modules and types. Eventually, combined cycle dynamics were modeled by [Dolezal et al, 1990 and Fujii et al, 1990].

Control of turbine power and speed [Dighe et al, 1976], power plant controller design [Åström et al, 1972 and Ray, 1980] and automation of single generator combined cycle plant [Baker et al, 1975] were investigated experimentally and theoretically.

Another area of research, [Galopin, 1994], was directed towards the swell effect that happens in the riser tubes and its effect on the drum inlet due to the resulting thermal stresses. **In this paper**, a mathematical model is presented to investigate the combined cycle dynamics with much less approximations and handling some of the cycle components with different solution approaches than previously applied. A proposed control scheme is also applied and tested with

optimized control parameters. Comparison with the operational steady state data of unit number 4 in Cairo South Combined Cycle Power Plant is also presented to test the model accuracy.

2. MATHEMATICAL MODELING

2.1. Combined cycle components

The unfired combined cycle (the most commonly used in the electric utility power generation) is modeled. It can be divided into eight modules: 1) Gas turbine simple cycle module, 2) Gas dampers module, 3) Superheater module, 4) Economizer module, 5) Steam drum module, 6) Downcomer-riser module, 7) Steam turbine module, and 8) Control system module.

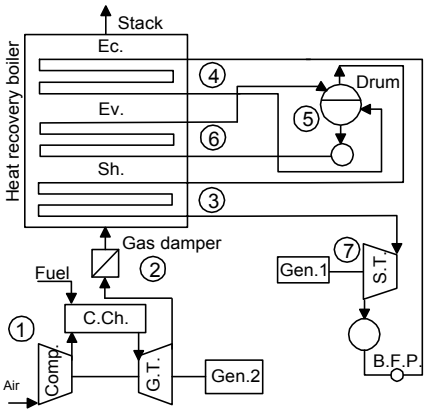

Fig.1 Schematic diagram for the CC modules

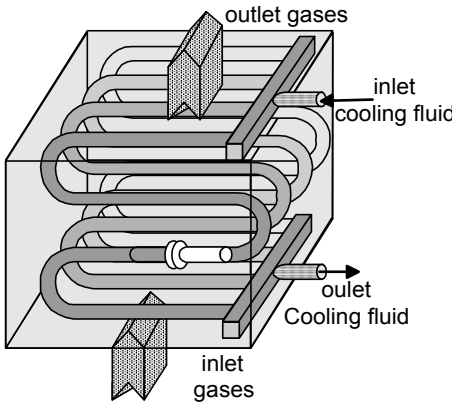

Fig.2 Counter-cross flow heat exchanger

Fig.1 shows a typical single pressure combined cycle in which the modules 1-7 are illustrated. These modules will be analyzed in detail for purpose of dynamic simulation of the combined cycle of unit 4 in Cairo South power plant, which the authors were able to obtain its data.

Common assumptions:

- The Gas turbine dynamics is not considered, as the gas turbine time response is relatively faster than that of heat recovery steam generator.
- Inertia of the hot gases is neglected; i.e. velocity changes take place instantaneously.
- The heat loss to the surroundings is neglected.

2.1.1 Heat Exchangers

The superheater and economizer are counter-cross flow heat exchangers, Fig.2. The cooling fluid flows through series of finned-tube banks normal to the direction of the heating fluid.

Moreover, the banks are parallel to each other and are connected by U-turns. The evaporator is purely cross flow. The tubes of the cooling fluid are vertical and perpendicular to the direction of the gas flow but without U-turns. The cooling fluid in the economizer is subcooled water but in the evaporator is wet steam while in the superheater is superheated steam. In all exchangers, the heating fluid is the gas-turbine exhaust gases. Considering the control element, Fig. 3, the energy equations (in x-y plane, neglecting temperature variation in the third dimension) for gas, fluid and metal are:

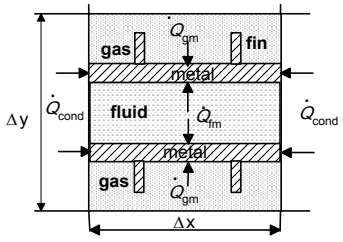

Fig.3 A finite element in x-y plane

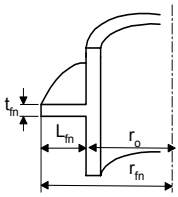

Fig.4 Circomferential fin of rectangular profile

Gas side

$$\frac{\partial T}{\partial t} + \gamma u_g \frac{\partial T}{\partial y} = \frac{-\dot{Q}_{gm}}{\rho_g V_g c_v} + \frac{\lambda_g}{\rho c_v}\left(\frac{\partial^2 T}{\partial y^2}\right) \tag{1}$$

Waterside

$$\frac{\partial T}{\partial t} + u_f \frac{\partial T}{\partial x} = \frac{-\dot{Q}_{fm}}{\rho_f V_f c_p} + \frac{\lambda_f}{\rho_f c_p}\left(\frac{\partial^2 T}{\partial x^2}\right) \tag{2}$$

The metal element is treated as a lumped system since Biot number is less than 0.1.

Metal side

$$\frac{\partial T}{\partial t} = \frac{\dot{Q}_{gm} + \dot{Q}_{fm}}{\rho_m V_m c_m} + \frac{\lambda_m}{\rho_m c_m}\frac{\partial^2 T}{\partial x^2} \tag{3}$$

The heat transferred within the element by convection from the gas or the fluid to the metal:

$$\dot{Q}_{gm} = A_o h_{gm}(T_g - T_m) \tag{4}$$

$$\dot{Q}_{fm} = A_i h_{fm}(T_f - T_m) \tag{5}$$

The convection heat transfer coefficient, h, is estimated, from the empirical formulae reported in [Holman, 1986] and [Stultz, 1992]:

a) For the cooling fluid flowing inside tubes in the range 0.5<Pr<100, which covers all fluids in boiler analysis:

$$h_{fm} = 0.023\frac{\lambda}{D_i}(\mathrm{Re})^{0.8}(\mathrm{Pr})^{0.4} \tag{6}$$

b) For the heating fluid flowing across in-line tubes:

$$h_{gm} = a\frac{\lambda}{D_o}(\mathrm{Re})^b(\mathrm{Pr})^{0.33} \tag{7}$$

The constants a & b are obtained from [Holman, 1986] according to the tubes configuration. Note that A_o in Eq. (4) is the sum of the outer tube and effective fin areas as will be shown.

2.1.2 Heat Transfer from Fins:

Assuming circular ring fins, Fig.4, instead of spiral ones, the effective heat transfer area is:

$$A_{fn,Effective} = A_{fn,Total}.\eta_{fn} \tag{8}$$

The following equation of fin efficiency fits the data of [Holman, 1986], within the range of interest, with good accuracy:

$$\eta_{fn} = 1 - 0.45\frac{(L_c)^{1.5}}{\sqrt{\lambda_{fn}.A_m}}\sqrt{h_{gm}} \tag{9}$$

Where $L_c = L_{fn} + 0.5t_{fn}$ & $A_m = t_{fn}.L_c$

2.1.3 Numerical solution of energy equation:

The x-y plane is divided into small meshes of lengths Δx and Δy, Fig.5. An implicit backward-central finite difference scheme is applied to ensure stable solution. The discretization equation for equation (1), as an example, is:

$$T_{i,j}^{t+1} = (aT_{i,j+1}^{t+1} + bT_{i,j-1}^{t+1} + sT_{m,i,j}^{t+1})/a_p \tag{10}$$

Where

$$a = \left[\frac{\lambda_g \Delta t \Delta x}{\rho_g c_v V_e}\right]_{i,j}^{t+1}, \quad b = \left[\frac{\Delta t\, \dot{m}_g\, \gamma}{V_e N_x N_r \rho_g}\right]_{i,j}^{t+1} + a$$

$$s = \left(\frac{\Delta t A_o h}{V_e \rho_g c_v}\right)_{i,j}^{t+1}, \quad a_p = 1 + a + b + s$$

$$A_o = \pi d_o \Delta x + \frac{\pi}{2}(d_{fn}^2 - d_o^2)N_{fn}\eta_{fn}, \quad V_e = \Delta x\overline{\Delta y}^2 - \frac{\pi}{4}d_o^2\Delta x \quad N_x = \frac{L}{\Delta x}, \quad N_r = \text{Number of tubes per row}$$

In counter-cross flow heat exchanger, the gas temperature varies in the x-y plane, while the fluid temperature varies in x-direction only. Therefore there must be a way to match the gas element with the fluid element passing through it. A proposed mesh numbering is suggested in Fig. 5 by which the gas temperature looks to vary in x-direction as the fluid does. The fluid elements follow the flow direction in a zigzag path so that the x-direction is reversed from row

to row. The transformation equations given below are proposed to assign any gas element in x-y plane:

Note that the first and last rows are gas-boundary elements. The following example illustrates the application of these equations to element (3, 4):

$$K_f = 5.(4-1) = 15$$

$$J = N(3,4) = 15+3 = 18$$

$$J-1 = N(3,3) = 15-3+1 = 13$$

$$J+1 = N(3,5) = 15-3+1+2x5 = 23$$

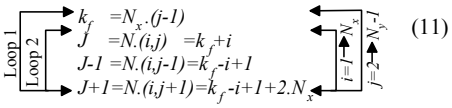

(11)

This agrees with the numbers shown in Fig.5.

Hint: This arrangement was originally devised for parallel-cross flow, which has reversed fluid ends. It is still valid for counter-cross flow but the fluid velocity should be substituted with negative sign in the fluid energy equation.

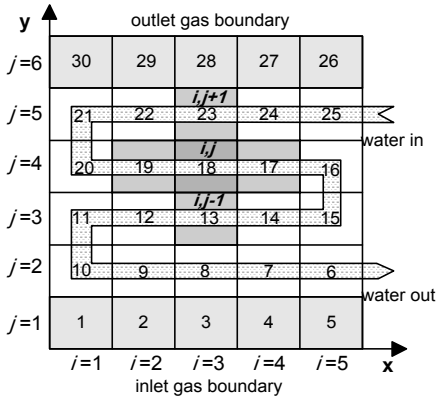

Fig.5 Proposed meshes distribution (N_x=5, N_y=6)

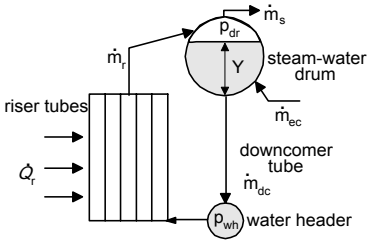

Fig.6 Drum and downcomer-riser loop

2.1.4. Boundary conditions

Inlet water, steam and gas temperatures are always known, while their outlet temperatures are obtained from linear extrapolations. For the counter-cross flow exchanger elements:

Gas: $T_g(i,N_y) = T_g(i,N_y-1),\ \ i=1 \rightarrow N_x$

Fluid: $T_f(N_x,2) = T_f(N_x+1,2)$ (Fictitious point)

The riser heat exchanger, which is cross flow, is treated as one-dimension. Its fluid equation needs not to be solved since the fluid temperature is assumed constant and equal to the saturation temperature corresponding to the drum pressure.

2.2. Steam-water Drum and Downcomer-riser

The drum and downcomer-riser loop, illustrated in Fig.6, comprises the steam-water drum, the downcomer tubes, the water header, and the riser tubes. The subcooled water flows from the economizer tubes to the bottom of the drum. As the riser tubes receive heat, the water-steam mixture, inside the tubes, rises up naturally to the drum while the water, in the drum, descends in the downcomer tubes. This process results in a saturated-steam generation flowing out of the drum. The governing equations for each component in the loop will be discussed hereafter.

2.2.1 Downcomer

From the momentum equation:

$$\frac{L_{dc}}{A_{dc}}\frac{d\dot{m}_{dc}}{dt} = (p_{dr} - p_{wh}) + \frac{gL_{dc}}{v_{dc}} - \frac{\dot{m}_{dc}^{2} v_{dc}}{2.A_{dc}^{2}}(\xi + f_{dc}\frac{L_{dc}}{D_{dc}}) \tag{12}$$

The water specific volume is a function of the drum pressure according to the given polynomial:

$$v_{dc} = \sum_{i=1}^{n} a_i p^{n-i}$$

2.2.2 Riser

Similarly, from the momentum equation:

$$\frac{L_r}{A_r}\frac{d\dot{m}_r}{dt} = (p_{wh} - p_{dr}) + \frac{\dot{m}_{dc}^{2} v_{dc}}{A_r A_{dc}} - \frac{gL_r}{v_r} - \frac{\dot{m}_r^{2} v_r}{2A_r^{2}}(2 + \xi + f_r\frac{L_r}{D_r}) \tag{13}$$

From the energy equation:

$$\frac{du_r}{dt} = \frac{v_r}{A_r L_r}(\dot{Q}_r + \dot{m}_{dc} h_{dc} - \dot{m}_r h_r - u_r \frac{dM_r}{dt}) \tag{14}$$

Where $$\dot{Q}_r = -\Sigma \dot{Q}_{fm} \tag{15}$$

From the mass balance:

$$\frac{dM_r}{dt} = (\dot{m}_{dc} - \dot{m}_r) \tag{16}$$

From the state equations:

$$x_r = (u_r - u_f)/u_{fg} \tag{17}$$

$$v_r = xv_g + (1-x)v_f \tag{18}$$

$$h_r = u_r + p_{dr}v_r \tag{19}$$

Equations (12-16) are integrated by Euler's exiplicit method and then solved with equations (17-19) to obtain the new values of $\dot{m}_{dc}, \dot{m}_r, u_r, x_r$ and p_{wh}. The heat transfer rate in Eq.(15) is obtained from the sumation of heat transfer rates over the riser elements as disscused earlier.

Assumptions for downcomer-riser loop:

- At any time interval, the water in the downcomer is assumed saturated water, corresponds to the drum pressure, instead of subcooled. This means that instantaneous evaporation takes place in the riser when drum pressure changes.
- Vapor and liquid velocities in the riser are identical.

2.3. Steam-water drum

The drum steam-water mixture is treated as a lumped system, at the saturation temperature corresponding to its pressure, to avoid the complexity resulting from the calculations of condensation as well as evaporation rates accompanied with the pressure changes. Referring to Fig.6, the mass balance of the drum results in:

$$\frac{dM_{dr}}{dt} = \dot{m}_{ec} + \dot{m}_r - \dot{m}_s - \dot{m}_{dc} \tag{20}$$

From the energy balance:

$$\begin{aligned}\frac{du}{dt} = \frac{1}{M_{dr}}(&\dot{Q}_{mf} + \dot{m}_{ec}h_{ec} + \dot{m}_r h_r \\ &- \dot{m}_s h_s - \dot{m}_{dc}h_{dc} - u\frac{dM_{dr}}{dt})\end{aligned} \tag{21}$$

Where $\dot{Q}_{mf} = A_{dr}h(T_m - T_f)$

Top

The relation between *dp*& du is derived as follows: Since $u = u_f + x_{dr} u_{fg}$

Differentiating both sides with resect to time and substituting for $d\phi/dt$ as $d\phi/dp.dp/dt$ (ϕ could be any property),

$$\frac{du}{dt} = du_{fg}\frac{dp}{dt} + u_{fg}\frac{dx_{dr}}{dt} \tag{22}$$

Where $$du_{fg} = (1 - x_{dr})\frac{du_f}{dp} + x_{dr}\frac{du_g}{dp}$$

Since $v_{dr} M_{dr} = V_{dr}$, then differentiating both sides w.r.t. time, considering V_{dr} as constant, results in:

$$\frac{v_{dr}}{M_{dr}}\frac{dM_{dr}}{dt} = -dv_{fg}\frac{dp}{dt} - v_{fg}\frac{dx_{dr}}{dt} \tag{23}$$

Where $$dv_{fv} = (1 - x_{dr})\frac{dv_f}{dp} + x_{dr}\frac{dv_g}{dp}$$

Solving Eqs. (22 & 23), the final relations are:

$$\frac{dp}{dt} = \frac{\dfrac{du}{dt} + \dfrac{u_{fg}}{v_{fg}}\dfrac{v_{dr}}{M_{dr}}\dfrac{dM_{dr}}{dt}}{du_{fg} - \dfrac{dv_{fg}}{v_{fg}}u_{fg}} \tag{24}$$

$$\frac{dx_{dr}}{dt} = \frac{\dfrac{du}{dt} + \dfrac{du_{fg}}{dv_{fg}}\dfrac{v_{dr}}{M_{dr}}\dfrac{dM_{dr}}{dt}}{u_{fg} - \dfrac{v_{fg}}{dv_{fg}}du_{fg}} \tag{25}$$

Refer to Fig.7, the water level time derivative can be obtained from:

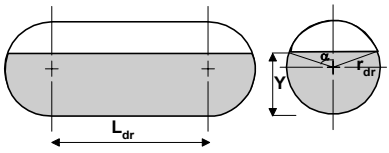

Fig.7 Longitudinal and cross section of the drum

$$V_w = V_{dr} - \{L_{dr}[\alpha r_{dr}^2 - (y - r_{dr})r_{dr}\sin\alpha] + \pi(2r_{dr} - y)^2[r_{dr} - \frac{(2r_{dr} - y)}{3}]\}$$

Top

Differentiating this equation w.r.t. time yields:

$$\frac{dY}{dt} = \frac{dV_w}{dt} / [2L_{dr}\sqrt{2y.r_{dr} - y^2} + \pi y(2r_{dr} - y)] \tag{26}$$

The water volume derivative can also be obtained:

Since

$$V_w = \frac{1 - x_{dr}}{\rho_w} M_{dr}$$

$$\frac{dV_w}{dt} = \frac{1}{\rho_w}[(1 - x_{dr})\frac{dM_{dr}}{dt} - M_{dr}\frac{dx_{dr}}{dt} - V_w\frac{d\rho_w}{dt}] \tag{27}$$

Equations (21& 24-27) are solved together by Euler's explicit method to obtain the drum pressure, level and dryness fraction. Various properties and their derivatives are obtained from least squared polynomial equations, which fit the steam data.

Assumptions for steam-water drum:

- There is no temperature gradient in both the vapor and liquid phases in the drum, and the temperature is always the saturation temperature corresponding to drum pressure.
- The heat loss to the atmosphere is neglected.

2.4. Steam Turbine

2.4.1. Thermodynamics of steam turbine

The steam turbine power is obtained from:

$$P_{st} = \dot{m}_s(h_s - h_{cond})\eta_{st} \tag{28}$$

Where $h_{cond.} = h_f + x_{cond}(h_g - h_f)|_{p_{cond}}$ and

$$x_{cond} = \frac{(s_{cond} - s_f)}{s_{fg}}\Big|_{p_{cond}}$$

The enthalpy and entropy of the superheated steam are obtained from two-dimensional least square equations, functions of pressure and temperature, specially developed for this work.

$$h_s = a_0 + \sum_{i=1}^{n} a_i T^{m-i} + \sum_{j=1}^{n} b_j p^{m-j} + \sum_{i=1}^{n-1}\sum_{j=1}^{n-i} c_{i,j} T^{m-j-i} p^j \tag{29}$$

$$s_s = d_0 + \sum_{i=1}^{n} d_i T^{m-i} + \sum_{j=1}^{n} e_j p^{m-j} + \sum_{i=1}^{n-1}\sum_{j=1}^{n-i} f_{i,j} T^{m-j-i} p^j \tag{30}$$

The coefficients are given in the appendix.

Top

2.4.2. Shaft speed dynamic:

The turbine shaft speed is a function of the turbo-alternator rotor self-inertia and the difference between the generated power and the load demand.

$$J_{st}\frac{d\omega}{dt} = P_{st} - P_l\,, \qquad J_{st} = M_{st}.R_{st}^2 \tag{31}$$

Assumptions for steam turbine:

- The steam turbine dynamics is just the rotor dynamics due to the inertia of the turbine-generator.
- The following effects are not considered:
  Mass or heat storage in fluid, heat loss to atmosphere, extractions, metal temperatures, and sealing steam.

2.5. Control Loops

The present work divides the control system of the steam part of a combined cycle unit into three integrated control loops; each of them relies upon the action of PID controllers. The first control loop controls the gas damper's position, which determines the mass flow rate of the flue gases entering the heat recovery steam generator. The second one controls the turbine steam valve's position, which determines the mass flow rate of the steam entering the steam turbine. The third one controls the feed water valve position, which determines the inlet water mass flow rate to the steam-water drum.

There are three control strategies to control the aforementioned loops; the single-element, the two -elements, and the three-elements. The three- elements, however is adapted here because of its effectiveness in controlling plant parameters.

2.5.1. PID controller

The control action is the resultant of the Proportional, Integral and Derivative actions responding to present, past and anticipated errors respectively. The controller equation is:

$$G_c = k_p\left(E_t + \frac{1}{T_i}\int_0^t E_t.dt + T_d\frac{dE_t}{dt}\right) \tag{32}$$

The velocity form of the discrete PID controller is, [see Sigeru et al, 1995]:

$$\begin{aligned}\Delta G_c = k_p\{&E_t - E_{t-\Delta t} + \frac{\Delta t}{2T_i}(E_t + E_{t-\Delta t}) \\ &+ \frac{T_d}{\Delta t}(E_t - 2E_{t-\Delta t} + E_{t-2\Delta t})\}\end{aligned} \tag{33}$$

Following is the application of Eq.(33) to the three-element control loop.

2.5.2 Three-element control system

Referring to Fig.8, the gas damper controller is actuated by a control signal depending on the corrective action of two variables. The steam and water valves controllers are actuated by control signals depending on the corrective action of three variables.

2.5.2.1. Gas damper position control loop

The error between the transient drum pressure and its reference value is summed with the modified error resulting from the difference between the power demand and the power generated. The resultant error value passes through a PID controller, to determines the gas damper position.

$$E(A_{gd}) = (p_{dr,r} - p_{dr}) + k_{P,\dot{m}_g} \frac{(P_r - P)}{P_r}$$

$$\Delta A_{gd} = \Delta G(E(A_{gd})) \tag{34}$$

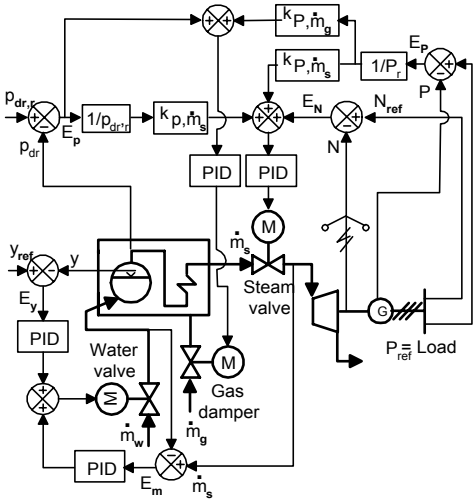

Fig. 8 Three-element control loop

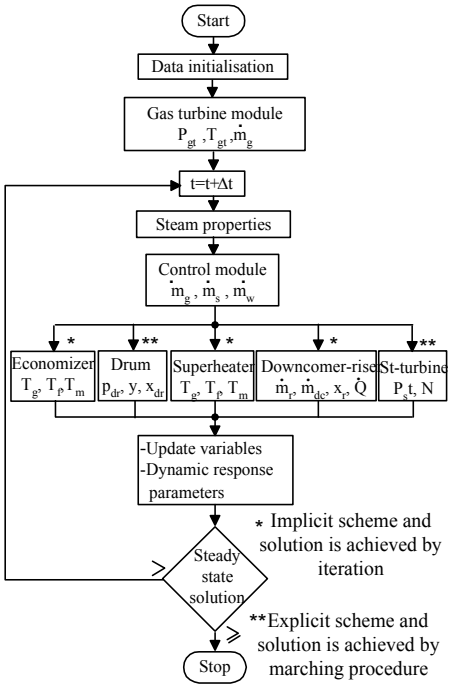

Fig.9 Flowchart

2.5.2.2 Steam valve position control loop

The error is the sum of the errors in speed, power and pressure.

$$E(A_{sv}) = N_r - N + k_{P,\dot{m}_s} \frac{P_r - P}{P_r} + k_{p,\dot{m}_s} \frac{p_{dr,r} - p_{dr}}{p_{dr,r}}$$

$$\Delta A_{sv} = \Delta G(E(A_{sv})) \tag{35}$$

2.5.2.3. Water valve position control loop

The error between the transient value of the drum water level and its set value is passed through a PID controller giving the control action due to level transients. The error between the steam and the water mass flow rates is passed through a second PID controller giving the control action due to the difference in mass flow rates (this overcomes the problem of long settling time resulting from the adverse effect of swell and shrink). These two control actions are summed together to determine the feed water valve position. The reason for using the second PID controller is that when a single PID controller is applied on the sum of the aforesaid errors for drum water level and mass flow rates it sometimes leads to an offset in the drum water level from its set value. This happens when the values of the two errors are equal but with opposite signs. This causes the resultant error signal going out from the summing point to the PID controller to be of zero value keeping the feed water valve at its position with an offset.

$$E(A_{wvy}) = y_r - y, \qquad E(A_{wvm}) = \dot{m}_s - \dot{m}_w$$

$$\Delta A_{wv} = \Delta G(E(A_{wvy})) + \Delta G(E(A_{wvm})) \tag{36}$$

Finally, Eqs. (34-36) are used to obtain the mass flow rates gas, steam and water:

$$\dot{m}_g = constant \times A_{gd} \tag{37}$$

$$\dot{m}_s = constant \times A_{sv} \times \rho_s \tag{38}$$

$$\dot{m}_w = constant \times A_{wv} \sqrt{2 \times \rho_w \times (p_{fp} - p_{dr})} \tag{39}$$

Where all areas are obtained from their summation over the time plus the initial area at zero time.

2.6. Overall solution

The equations of the eight modules of the combined cycle were solved together step by step through a computer program written in FORTRAN language. The solution step was optimized at 0.1 s. The flow chart, in Fig. 9, shows the major tasks of the program.

3. RESULTS

The simulation is applied to the Unit 4 in Cairo South Combined Cycle Power Plant. The maximum continuous rating is 180 MW; one third of it is produced by the steam turbine. The main design parameters of the plant are shown in Table 1.

Table 1. Design parameters of simulated plant

	Super heater	riser	Econo-mizer	Down comer
No. of tubes/row	60	60	60	3
No. of tube rows	8	16	12	1
Tube length, m	14.94	14.94	14.94	14.94
Tube outer diam. ,m	.0508	.0508	.0508	.22
Tube inner diam. ,m	.0471	.0478	.0473	.20
No. of fins per meter	236	236	228	0
Fins thickness, mm	1.27	1.27	1.27	0
Fins length, mm	12.7	19.05	18.4	0
H.P. Drum length, m				7.188
H.P. Drum inside diameter, m				2.1336
Gas Turbine Air/fuel ratio				54:1
Lower calorific value of G.T. fuel, kJ/kg				45795
Gas turbine pressure ratio				11:1
Ambient temperature, ^{o}C				18.3

Table 2. Recorded and simulated data for steady state performance of Unit 4 combined cycle power plant

	Recorded	simulated
H.P. steam mass flow rate, kg/s	48.7	47.7
L.P. steam mass flow rate, kg/s	8.4	8.6
HRSG gas mass flow rate, kg/s	404	414
H.P. Superheater outlet temp,^{o}C	511	523
H.P. Economizer outlet temp.,^{o}C	265	263
HRSG stack gas temperature, ^{o}C	106	107

Table 3. Reference parameters

H.P. drum pressure, bar	65
H.P. drum level, m	1.4
Steam turbine speed, rpm	3000

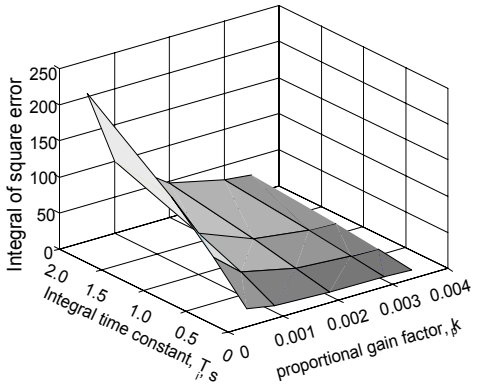

Fig. 10 Control parameters optimzation for steam valve controller

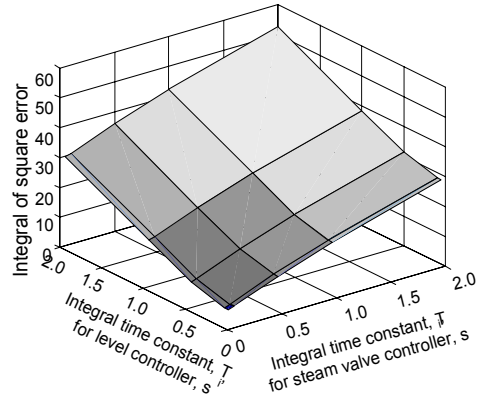

Fig. 11 Control parameters optimzation for level and steam valve controller

Table 2. shows a summary of this comparison. The model results agree very closely with the field data with maximum deviation of less than 2.5%. So many cases of sudden change of load (decrease and increase) were performed. The control parameters were optimized according to the ITSE (Integral time of square error) method, settling time and maximum oversoot. Fig. 10 shows, for the steam valve controller, that ITSE is reduced by either increasing the

proportional gain or decreasing the integral time constant. Similar trends can be shown for other PID control parameters, see Fig. 11.

A case study of sudden 50% decrease of load for a period of 200 seconds followed by sudden increase to the initial load for another 200 seconds was performed. This load cycle aimed at investigating the time response of the steam pressure and water level in the drum, speed and load of the steam turbine, mass flow rates in the cycle and many other parameters. The figures that will be shown later are for high-pressure side of the cycle only.

As the load demand is suddenly decreased or increased, the control system responds by either closing or opening the steam valve and the gas damper to reduce or raise the turbine power. However, the power difference between the demand and the turbine output, due to time lag, causes the turbine to run faster or slower than the reference speed for some time. The control action continues to adapt the steam and gas flow rates so that the power difference is diminished and hence the turbine speed is settled down close to the reference state, see figures 12, 15 & 20. The maximum speed variation corresponding to 50% load increase, Fig. 12, does not exceed 1.5% of the reference speed. The corresponding settling time is less than 100s. During the load cycle, the drum pressure, Fig. 13, responds in an opposite manner to the load change due to the rapid decrease or increase of the steam flowing out of the drum, Fig. 15. The drum water level and pressure are inversely related as shown in Fig. 13. Meanwhile, the water flow rate entering the drum compensates for the water level, Fig. 15. The effect of decrease or increase of the gases mass flow rate is strongly reflected on the riser and downcomer mass flow rates and hence the riser dryness fraction as shown in figures 14 & 16. The drum dryness fraction is inversely influenced by the drum water level as shown in Fig. 16.

The temperature time response takes longer time to reach the steady state compared to the aforementioned parameters. Figures 17-19 show the temperature variation of gases, metal and steam or water in the superheater, riser and economizer during the load cycle. The outlet temperature of the steam in the superheater at part load, as shown in Fig.17, is a little higher than that of full load. The metal temperature in the economizer exhibits a big overshoot in a relatively short time as load increases from part load to full load, Fig.19. This may generate sudden thermal stresses on the tubes material which should be taken into consideration during the design stage. The gas temperature in the chimney is shown in Fig. 20 to take about 1200s to reach the steady state. It can also be noticed that the chimney temperature at part load is less than that of full load condition. Also the gas temperature at chimney exhibits overshoot as high as twice as the steady state value at the point where sudden increase of load is applied.

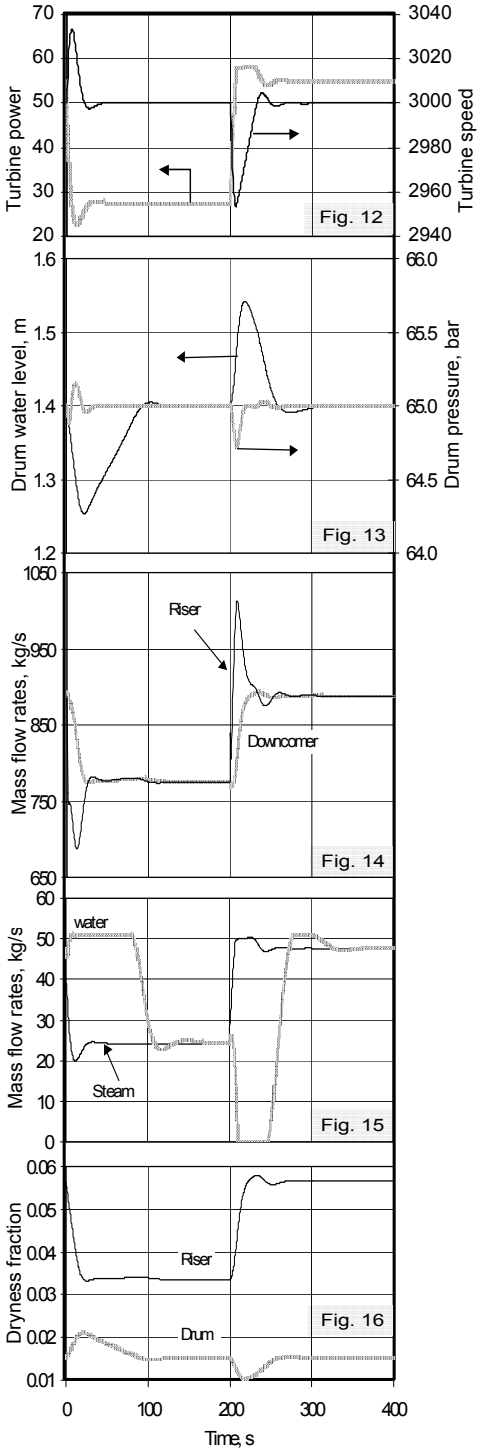
Turbine power
Turbine speed
Fig. 12
Drum water level, m
Drum pressure, bar
Fig. 13
Mass flow rates, kg/s
Riser
Downcomer
Fig. 14
Mass flow rates, kg/s
water
Steam
Fig. 15
Dryness fraction
Riser
Drum
Fig. 16
Time, s

Top

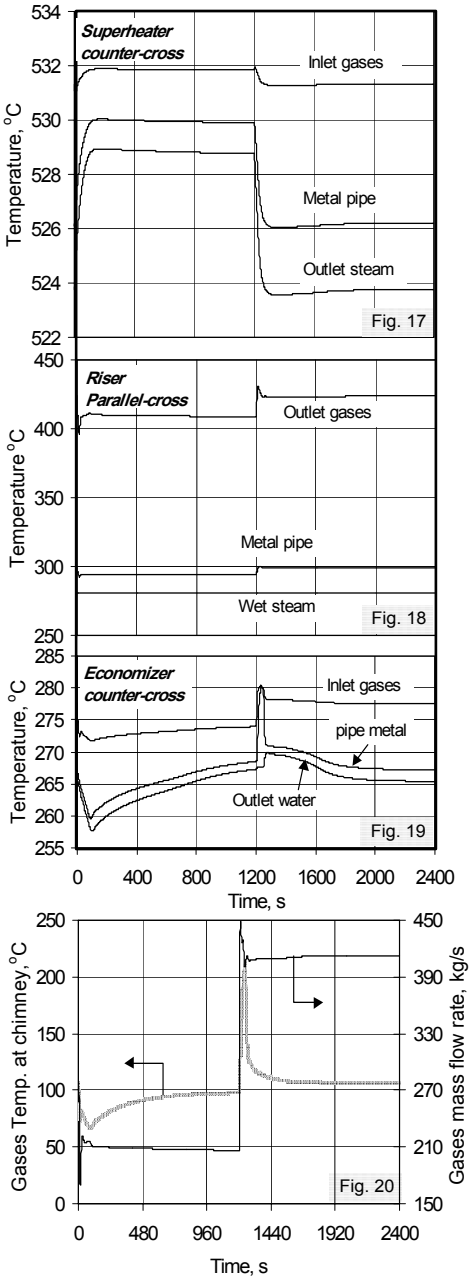
Superheater
counter-cross
Inlet gases
Metal pipe
Outlet steam
Temperature, °C
534
532
530
528
526
524
522
Fig. 17
Riser
Parallel-cross
Outlet gases
Metal pipe
Wet steam
Temperature °C
450
400
350
300
250
Fig. 18
Economizer
counter-cross
Inlet gases
pipe metal
Outlet water
Temperature, °C
285
280
275
270
265
260
255
Fig. 19
0
400
800
1200
1600
2000
2400
Time, s
Gases Temp. at chimney, °C
250
200
150
100
50
0
Gases mass flow rate, kg/s
450
390
330
270
210
150
Fig. 20
0
480
960
1440
1920
2400
Time, s

4. CONCLUSIONS

The dynamics of the combined cycle, which comprises gas turbine and steam cycle, is construed by the behaviour of the steam part owing to the large stored energy in water, steam and metal contained in their components. This work achieved the following major contributions:

i- An improved mathematical model comprises:

- Numerical solution of the unsteady one-dimensional energy equation of gas, metal and steam (or water) for both parallel and counter cross flow heat exchangers. A special mesh arrangement was proposed by which the heat exchanger tubes have considered as elongated to a single long tube while assuring the solution accuracy by maintaining the conditions of each mesh and its neighboring ones as their original state. An Implicit backward-central finite difference scheme was implemented to assure stability and solution was achieved by iteration.

- Development of special accurate two-dimensional least square equations for the superheated steam properties as functions of pressure and temperature. This provides accurate properties with much less time than the common procedures based on interpolations techniques.

- Careful treatment of the dynamic equations of the natural circulation in the downcomer-riser system.

- Complete deduction of the dynamic equations of steam-generating unit.

ii- Proposal and adaptation of a reliable three-element control scheme by which the plant was fully controlled under sudden increase or decrease of load. The velocity form of the discrete PID control equation was implemented and the control parameters were optimized according to the ITSE. Hence the settling time and the overshoot or undershoot, particularly for the steam turbine speed and power, could be minimized.

REFERENCES:

1. Åström, K. J., and Eklund, K., 1972, "A Simplified Non-Linear Model of a Drum Boiler-Turbine Unit," Int. J. Control, Vol. 16, No. 1, pp. 145-169.
2. Baker, J. M., Clark, G. W., Dolbec, A. C., and Patel, A. S., 1975, "Automation of multi-generator combined cycle plants," An ASME Publication, 75-PWR-23.
3. Carvalho, F. L., Coradie, F. H. D., Croft, Kuerten, D. G., H., and McDyer, F. J.,1991, "The Influence of Control System Design on the Dynamic Response Characteristics of Thermal Power Plants," Proceedings Institution of Mechanical Engineers., Vol. 205, Journal of Systems and

Control Engineering, 'Load Cycling, Plant Transients and Off-Design Operation' Siminar, London.

4. Chien, K. L., Ergin, E. I., Ling, C., and Lee, A., 1958, "Dynamic Analysis of a Boiler," Trans. ASME, Paper No. 58-IRD-4, pp. 1809-1819.
5. Debelle, J., Foureau, A., and Vazquez, R., 1966 "Parametric Control of Boilers and Identification of Furnace Perturbation," Steam Boilers and Heat Exchangers, ASME, Session 10, Paper 10.C.
6. Dechamps, P. J.,1994, "Modeling the Transient Behaviour of Combined Cycle Plants," An ASME Publication, 94-GT-239, Presented at the International gas turbine and aero-engine congress and exposition, The Hague, Netherlands.
7. Dighe, A. S., Narasimhan, R., and Kamble, P. D., 1976, "Turbine-Boiler Modeling for Power System Dynamics Studies," Symposium on Power Plant Dynamics, India, pp. 282-293.
8. Divakaruni, S. M., and Hottenstine, R. D., 1990, "Assuring Benefits from Advanced Modeling of Fossil Power Stations," Mathematical Modeling and Computer Simulation of Processes in Energy Systems, Proceedings of the International Center for Heat and Mass Transfer, pp. 763- 777, Hemisphere Publishing Corp..
9. Dolezal, R., and Riemenschneider, G., 1990, "Dynamics of Cogeneration Plants (Combined Cycles)," Mathematical Modeling and Computer Simulation of Processes in Energy Systems, Proceedings of the International Center for Heat and Mass Transfer, pp. 539-559, Hemisphere Publishing Corp..
10. Eigner, H., 1966, "The Fundamentals of Heat Exchanger Dynamics with Special Attention to Double Tube Heat Exchangers," Steam Boilers and Heat Exchangers, ASME, Session 10, Paper 10.A.
11. Eklund, K., and Gutavsson, I.,1973, "Identification of Drum Boiler Dynamics," IFAC Symposium, 3rd Proceeding Pap., pp. 87-108, Part 1, The Hague/Delft, Neth., June 12-15.
12. Estrada, H., and Leeds, J. V., 1964, "Transient Response of Water Level in Recirculating Boilers and Steam Generators," An ASME Publication, 64-WA/PWR 3, presented at the ASME Winter Annual Meeting, N. Y., Nov. 29-Dec. 4.
13. Farber, E. A., 1951, "Investigation of Steam Separation in Boiler Drums Through Studies on a Model," Trans. ASME, Paper No. 50-F-25, pp. 247-256.
14. Fujii, T., Ohta, J., Ziang, A. Z., Kijima, K., and Kinka, T., 1990, "Dynamic Characteristics of Boilers in Combined Cogeneration Plants," Mathematical Modeling and Computer Simulation of Processes in Energy Systems, Proceedings of the International Center for Heat and Mass Transfer, pp. 561-572, Hemisphere Publishing Corp..
15. Galopin, J. F., 1994, "Dynamic Constraints on HRSG Drum Design," An ASME Publication, 94-GT-239, Presented at the International gas turbine and aero-engine congress and exposition, The Hague, Netherlands.
16. Holman, J. P., 1986, "Heat transfer", 6th Edition, McGraw-Hill Book company, USA.
17. Mesarovic,M. M., 1990,"A Mathematical Simulation Method for the Evaluation of Operational and Accidental Transients in Thermal Power Systems," Mathematical Modeling and Computer Simulation of Processes in Energy Systems, Proceedings of the International Center for Heat and Mass Transfer, pp. 599-607, Hemisphere Publishing Corp..

18. Nahavandi, A. N., and Batenburg, A., 1966, "Steam Generator Water Level Control," Steam Boilers, ASME, Session 16, Paper 16.A.
19. Ray, A., 1980,"Dynamic Modeling of Power Plant Turbines for Controller Design," Appl. Math. Modeling, Vol. 4, No. 2, pp. 109-112.
20. Schöne, A., 1966, "A Special Class of Transfer Functions for the Description of the Dynamic Behavior of Heat Exchangers," Steam Boilers and Heat Exchangers, ASME, Session 10, Paper 10.B.
21. Sigeru Omatu, Marzuki Khalid and Rubiyah Yusof, 1995, "Neuro-Control and its Applications," Springer-verlag London limited.
22. Stultz, S. C., Kitto, J. B., 1992, "Steam/its generation and use," 40th Edition, Babcock & Wilcox Company, a McDermott Company, Ohio, USA.
23. Usoro, P. B., and Wormley,D. N., 1983, "Mathematical Modeling of Fossil-Fueled Steam Power Plants Under Normal and Emergency Operating Conditions - Part I : Methodology," Proceedings of 5th Power Plant Dynamics, Control & Testing Symposium, USA.
24. Wang, Yu, Singh, K. P., Soler, A. I., and Iulianetti, K., 1991, "Transient Response of Large Inertia Cross Flow Heat Exchangers," ASME, International Power Generation Conference, San Diego.

Appendix

Coefficients of the two-dimensional least square equations (*n=4, m=n+1*) for the enthalpy (kJ/kg) and entropy (kJ/kg K) of the superheated steam. They are valid in the range of *10<p<100* bar:

A_0 = 0.2232423411E+04	$C_{1,2}$=-0.4566812971E-06	e_1 = 0.3583122300E-07
A_1 =-0.2251006839E-07	$C_{1,3}$= 0.8808462910E-07	e_2 =-0.9934230700E-05
A_2 = 0.3365725975E-04	$C_{2,1}$=-0.4038557664E-03	e_3 = 0.8530098417E-03
A_3 =-0.1731630672E-01	$C_{2,2}$= 0.4609439844E-03	e_4 =-0.1053202668E+00
A_4 = 0.5587198355E+01	$C_{3,1}$= 0.1803216960E+00	$f_{1,1}$= 0.5358877882E-09
B_1 = 0.1276617288E-06	d_0 = 0.5704100845E+01	$f_{1,2}$=-0.6936110346E-09
B_2 =-0.7599058231E-04	d_1 =-0.4373110825E-10	$f_{1,3}$= 0.2702712889E-09
B_3 =-0.1121216568E+00	d_2 = 0.6807799862E-07	$f_{2,1}$=-0.7331731091E-06
B_4 =-0.2801629105E+02	d_3 =-0.3942215429E-04	$f_{2,2}$= 0.6799019094E-06
$C_{1,1}$= 0.2986812930E-06	d_4 = 0.1320675721E-01	$f_{3,1}$= 0.3310164069E-03